

Spontaneous Unidirectional Loop Extrusion Emerges from Symmetry Breaking of SMC Extension

Andrea Bonato,^{1,*} Jae-Won Jang,² Kyoung-Wook Moon,² Davide Michieletto,^{3,4,†} and Je-Kyung Ryu^{2,‡}

¹*Department of Physics, University of Strathclyde, Glasgow, G4 0NG, UK*

²*Department of Physics and Astronomy, and Institute of Applied Physics, Seoul National University, Seoul, 08826, South Korea*

³*School of Physics and Astronomy, University of Edinburgh, Peter Guthrie Tait Road, Edinburgh, EH9 3FD, UK*

⁴*MRC Human Genetics Unit, Institute of Genetics and Cancer, University of Edinburgh, Edinburgh EH4 2XU, UK*

DNA loop extrusion is arguably one of the most important players in genome organization. The precise mechanism by which loop extruding factors (LEFs) work is still unresolved and much debated. One of the major open questions in this field is how do LEFs establish and maintain unidirectional motion along DNA. In this paper, we use High-Speed AFM data to show that condensin hinge domain displays a structural, geometric constraint on the angle within which it can extend with respect to the DNA-bound domains. Using computer simulations, we then show that such a geometrical constraint results in a local symmetry breaking and is enough to rectify the extrusion process, yielding unidirectional loop extrusion along DNA. Our work highlights an overlooked geometric aspect of the loop extrusion process that may have a universal impact on SMC function across organisms.

DNA loop extrusion by structural maintenance of chromosome (SMC) complexes has emerged as a universal organizing principle for chromosomes [1–7]. For instance, it is now well established that in eukaryotes, cohesin complexes are involved in shaping “topologically associating domains” (TADs) during interphase [8, 9], while condensin complexes direct the establishment of the cylindrical structure of mitotic chromosomes [10].

SMC complexes have a ring-like structure, composed by a SMC dimer and an intrinsically disordered kleisin subunit. The SMC dimer is formed through the so-called “hinge” while the kleisin subunit is bound to the ATPase domain of each SMC (Fig. 1a). In the case of yeast condensin, there are putative additional DNA binding sites in the hinge, dimerized heads, Ycg1/Brn1 and Ycs4/Brn1 for DNA anchoring [11]. Despite the wealth of structural data, there is still contrasting evidence regarding the precise topology and mechanics of loop extrusion process.

Among the most debated features of loop extrusion are the motoring action of the hinge and the origin of the unidirectional motion [12–15]. Recent structural studies have suggested that SMC uses conformational changes between a hinge-released state – where the hinge is extended away from the heads – and a hinge-engaged state – where the hinge is in proximity of the heads, in order to drive the motion in a “scrunching”, and ATP-dependent, fashion [7, 16, 17] (Fig. 1a, b). The scrunching model predicts that following dimerisation of the SMC heads (due to ATP-binding), the coiled-coil arms fold to bring the hinge closer to the heads. Following ATP-hydrolysis, the heads are released and the hinge extends again [14, 16, 18]. During this step, the positively charged extended hinge may search for a 3D

proximal (but not necessarily 1D contiguous) DNA segment to grab and to subsequently bring close to the heads in the following ATP-binding step [14, 19]. Whilst this model can elegantly explain the bypassing of other SMCs [20, 21] and large roadblocks [22, 23], it cannot explain unidirectionality. Indeed, during the search step, there is no guarantee that the hinge will grab onto a DNA segment ahead of the one that was reeled in the extruded loop in the previous ATP cycle. Thus, even within the scrunching model explaining the unidirectional motion of LEFs remains an outstanding problem in the field of SMC-driven DNA organisation.

To gain a better understanding of the origin of the unidirectional motion, we use High-Speed AFM (HS AFM) on yeast condensin [16]. We observed that the hinge domain typically extends in an orthogonal direction from the DNA-bound globular head domains, and we then hypothesised that this local (angular) symmetry breaking due to the structure of condensin could generate a geometric bias in the grabbing of new DNA segments. Thus, we computationally implemented a loop extrusion process with such geometric constrain, by modelling a 3D search constrained to lie within a solid angle, and we discovered that it spontaneously displayed rectified, unidirectional extrusion. Our findings suggest that a geometric symmetry-breaking mechanism, without the need to impose explicit topological constraints between the SMC complex and extruded DNA segment, could underlie the emergence of rectified, unidirectional loop extrusion by SMC proteins.

AFM reveals a preferred angle for hinge extension. –

We started from the hypothesis that the structure of SMC itself may present some geometric restrictions on

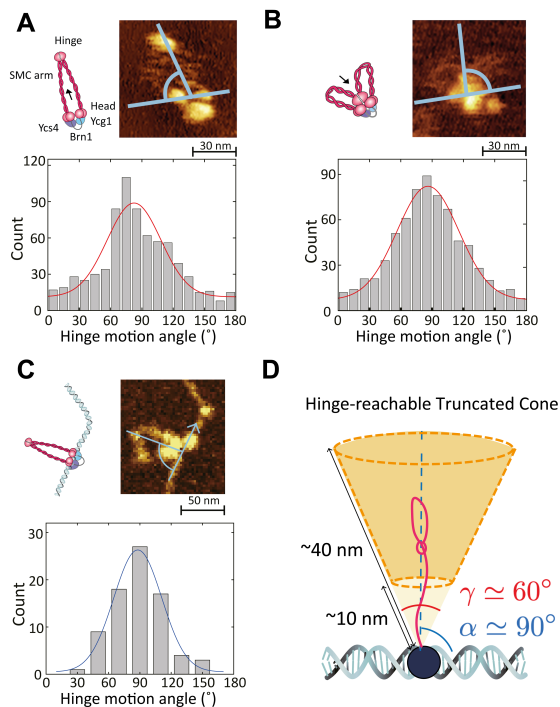


FIG. 1. Limited solid angle of hinge movement from the position of the SMC heads. **a-b.** Angle distributions of hinge-releasing **a.** and hinge-engaging movements **b.** respect to the line connecting two heads at the middle of two heads observed by HS AFM ($N = 727$ and 698 , respectively). **c.** Distributions of the angle between hinge and the central position of the globular domain with respect to tangential DNA line at the central positions of the globular domain analysed by dry-AFM images ($N = 79$). **d.** Sketch of the truncated cone hinge-reachable region determined by the AFM data.

its allowed conformations. Specifically, we argued that the hinge, connected to dynamic coiled-coil arms [18], largely determines the search of the DNA segment to be captured and reeled in the extruded loop. For this reason, we wanted to measure the possible geometric conformations assumed by a LEF, in order to quantify any restriction on the motion of the hinge. To do this, we performed and analysed High-Speed AFM (HS AFM) images of yeast condensin complex to obtain the typical position of the hinge with respect to the globular head domains [16] (Fig. 1). From the HS AFM movies we could identify two distinct globular domains: the hinge and the heads, linked together by semi-flexible arms (Fig. 1a). Furthermore, we were able to distinguish hinge-released and hinge-engaged states by measuring the distance of the hinge from the heads (see Fig. 1a-b and SI Fig. S4). Based on these, we measured the angles of hinge-releasing and hinge-engaging states, with respect to the line connecting two heads and from the middle point of two heads (Fig. 1a-b). In addition, to compare these angles with the anchoring angle of condensin with respect to the DNA, we analyzed dry-AFM images and measured the angle

of hinge extension with respect to the DNA-bound head domains (Fig. 1c).

We discovered that the hinge is most often extended orthogonally to the line joining the SMC heads (Fig. 1a-b). Even in absence of DNA, we measured that the angle distribution at which the hinge is extended and retracted is normally distributed for both hinge releasing ($83 \pm 26^\circ$) and engaging ($86 \pm 30^\circ$) steps. In addition, dry-AFM images of condensins that bound to DNA through head domains also showed vertical angle of the hinge-head line respect to DNA tangential direction ($88 \pm 23^\circ$) (Fig. 1c).

It is important to notice that our measurements are done on condensin complex absorbed on mica, i.e., in 2D. Thus, we argue that the angle distribution of the hinge extension would define a solid angle when the complex is allowed to move in 3D. Indeed, our results suggest that the hinge releases and engages orthogonally to both heads and DNA, forming a solid angle Ω defined by the width of the Gaussian distribution, $\gamma \approx 60^\circ$ (see Fig. 1d).

Based on the AFM results, we defined a hinge-reachable region for the scrunching model as a truncated cone with the estimated solid angle Ω (Fig. 1d). The maximum hinge extension is determined from the distribution of hinge-head distances in the hinge-released state (≈ 40 nm) while the minimum hinge extension is obtained as the hinge-head distance in the hinge-engaged state [16] (≈ 10 nm, see SI Fig. S4).

A LEF model with geometrically biased 3D search. –

In light of our HS AFM measurements, we propose a new geometrically-constrained scrunching model as follows: first, Ycg1/Brn1 anchors DNA with a “safety belt” mechanism [24] then the heads/Ycs4 connect the anchors to other part of DNA to extrude a loop (Fig. 2a). The motor action of the hinge is limited by the angle distribution we found in Fig. 1, and can grab DNA segments through the hinge, by extending the SMC arms at a fixed angle $\alpha \approx 90^\circ$ and with a certain width $\gamma \approx 60^\circ$ from the orientation of the bound DNA. After that the hinge grabs onto a new DNA segment, the ATP-binding-induced conformational change brings the grabbed DNA close to the heads/Ycs4 subunits. Finally, after ATP-hydrolysis, the heads/Ycs4 bind to the new DNA segment – thereby extending the extruded loop – and the hinge is then free to target a new DNA segment for the next round of DNA-loop extrusion (Fig. 2a).

To simulate this model, we implemented a coarse-grained loop extrusion process with a geometric constraint on the region that can be reached by the hinge. Specifically, we account for the connectivity of the anchor (Ycg1) to the heads (Smc2 and Smc4) via the kleisin subunit as beads connected by a harmonic bond; additionally, we impose that the search of the segment to reel in the extruded loop is to be performed within a solid angle around an axis orthogonal to the tangent of the SMC-bound DNA (Fig. 2b). When a segment of the coarse-grained polymer falls within a truncated cone

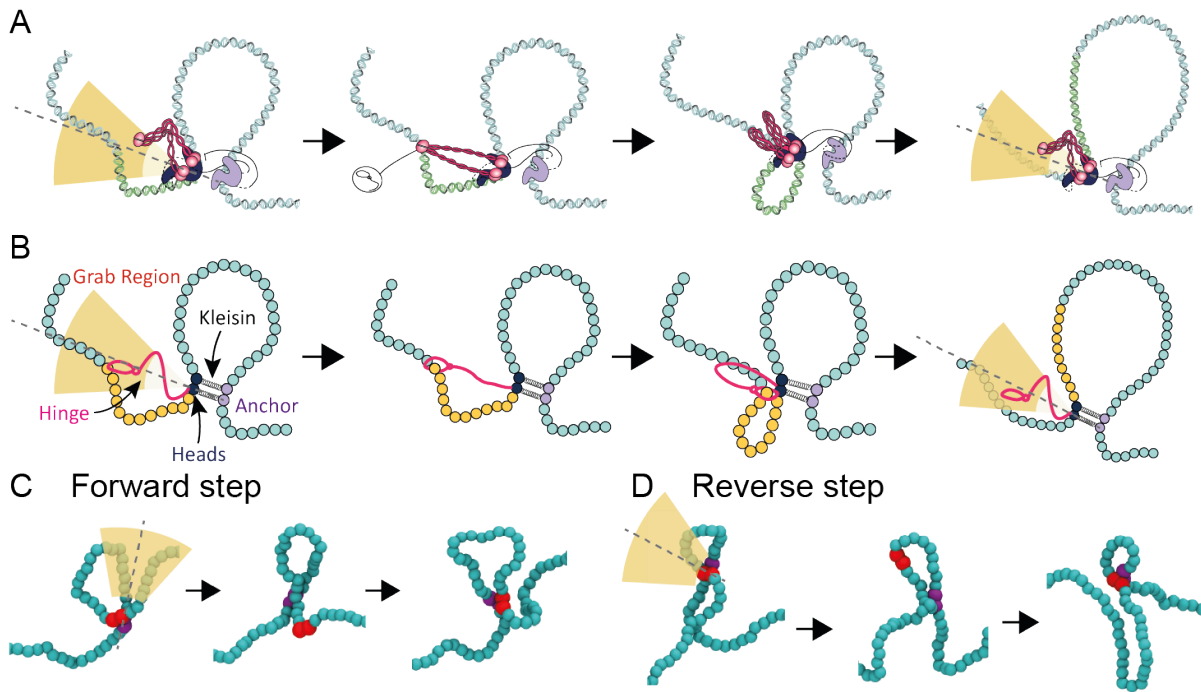


FIG. 2. **A model for loop extrusion with geometric constraints on hinge extension.** **a.** Schematics of a loop extrusion model where the hinge (red) is restricted to search for a DNA segment within a truncated cone. The segment is then bound to the SMC heads and reeled in the extruded loop, while the hinge returns to the search position. Throughout this process, one DNA segment is trapped at the anchor bound to the kleisin (purple). **b** Implementation of the model on a coarse-grained bead-spring polymer, where the heads and anchor are denoted with red and purple beads, respectively. The hinge is not explicitly modelled with a bead, but is accounted for by the geometrically restricted search region (yellow shaded area). The simulated loop extrusion displays both (c) forward and (d) backward steps.

formed by the solid angle Ω and within a certain Euclidean distance (10 and 40 nm) the position of the harmonic bond between anchor and heads is updated to grab onto the anchor and such new segment (see Fig. 2b). In turn, the harmonic spring connecting anchor and heads is temporarily extended and brings the new segment close to the anchor. Finally, the new segment is identified with the new position of the heads, the anchor remains at its original position, and the hinge is then returned free to search for a new segment to grab onto (again within the solid angle Ω). This process defines a full ATP-cycle and involves a 3D search of proximal DNA segments with a geometric constraint but no strict topological requirements.

The important difference of our work from previous models of loop extrusion [2–4, 14, 19, 25, 26] is that we do not impose the directionality of the extrusion *a priori*. The hinge can grab any segment ahead, or behind, the current 1D position of the heads. In fact, in our simulations we can observe backward extrusion steps, where the newly grabbed segment is *inside* the extruded loop, as shown in Fig. 2c, d. This move yields a reduction in the total length of the extruded loop and is also observed in experiments [27]. In addition, our model accounts for an additional spring to mimic the presence of the disordered kleisins attaching the anchor YcgI to the SMC heads (SI). This additional spring constrains

the relative rotation of the DNA segments bound to the heads and the anchor. This rotational constraints cannot otherwise be imposed if two beads are connected by a single spring [28]. The rotational constraint within the DNA-bound SMC complex is evident from structural cryo-EM data [11], where the bound DNA segments sit tightly within DNA-binding pockets near the heads, and that their juxtaposition within the SMC structure assume a well-defined angle [11]; this implies that SMC-bound DNA segments are likely to be restricted in their relative rotation.

Using this model, we performed a simulated loop extrusion on a bead-spring polymer with $N = 400$ beads of size $\sigma = 10$ nm. We then tracked the position of the anchor and heads, and defined an oriented extruded loop length as $l = n_a - n_h$, where n_a and n_h are the positions of the anchor and the heads; we discovered that, strikingly, the LEFs display growing loops with a clear sign of unidirectional motion. Since we do not hard-code directionality within the model, the LEFs in different replicas will start extruding in different directions. The interesting finding is that they display a tendency to maintain a rectified, unidirectional motion, once that the “left-right” symmetry has been broken (Fig. 3a).

To understand how this spontaneous rectification is due to the broken symmetry in the search step, we performed simulations with wider search angles up to restor-

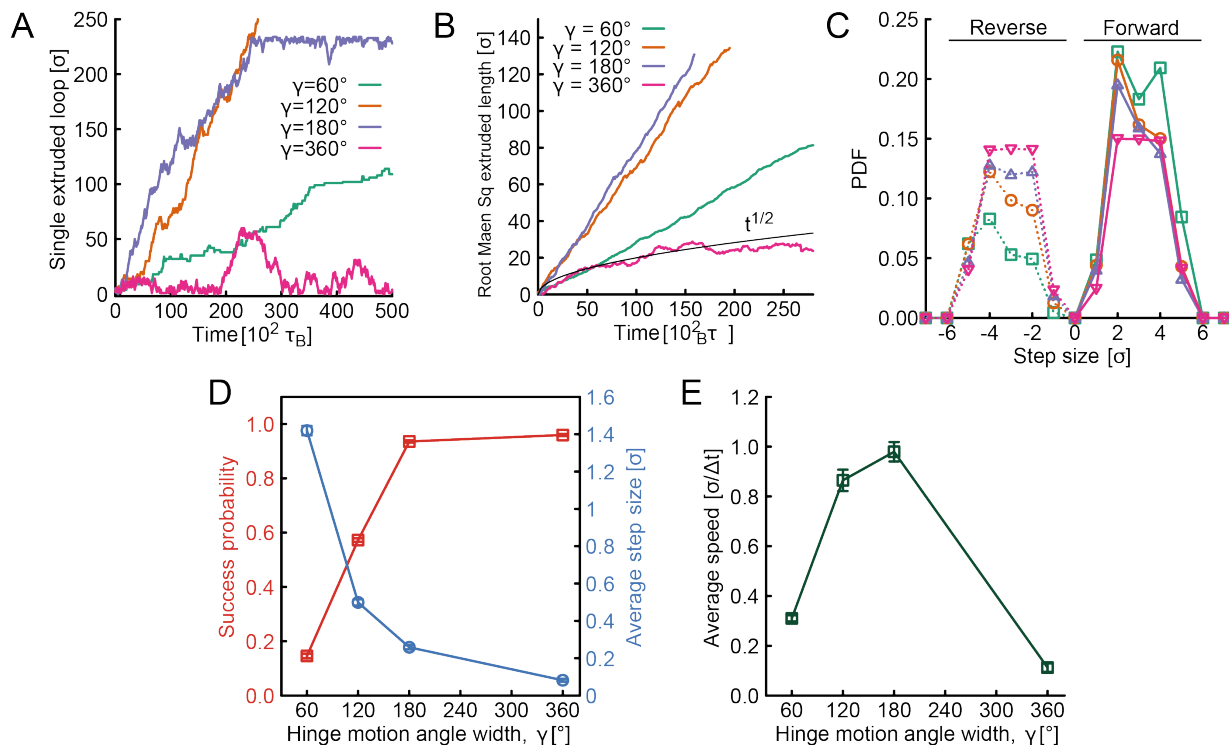


FIG. 3. **Unidirectional motion emerges from symmetry breaking.** **a.** Individual traces of simulated extruded loops as a function of time and with different hinge-search angles. **b.** Root mean squared extruded length as a function of time and for different hinge-search angles. The case where the search is allowed to occur on the full sphere $\gamma = 360^\circ$ yields a random walk scaling as $t^{1/2}$. **c.** Probability of step size as a function of the search angle. The narrower the angle, the more rectified the extrusion, i.e. the larger the forward/reverse ratio. **d.** Plot of the success probability and average step sizes as a function of the hinge search angle. These two quantities display a trade-off which yield an optimum of the extrusion velocity at $\gamma = 180^\circ$ search angles, as shown in **e.**

ing the full spherically symmetric search $\gamma = 360^\circ$. In the symmetric case, we do not observe unidirectional motion, instead we find that extruded loops shrink back, with a behaviour similar to a random walk (see Fig. 3a). To further characterise this process we took the root mean squared extruded length $\langle l \rangle = \langle [n_a - n_b]^2 \rangle^{1/2}$ and indeed found that the spherically symmetric case displayed a scaling $\langle l \rangle \sim t^{1/2}$, in line with a simple random walk (see Fig. 3b). Interestingly, we also noted that the cases with $60^\circ < \gamma < 360^\circ$ displayed faster linear growth than the case with $\gamma = 60^\circ$. Despite this, the distribution of step sizes clearly indicate that the case $\gamma = 60^\circ$ is the one that benefits from the greater rectification, i.e. the ratio forward/reverse steps is the largest. In other words, wider angles increase the probability of shorter and backward steps (Fig. 3c). In turn, this implies that the average step size – defined as $s = \sum_i [\text{sign}(i) S_i] / N$, where S_i is the i -th step size – is typically smaller for wider angles. The largest probability of large steps ~ 50 nm, which is in line with experiments [27], was seen for $\gamma = 60^\circ$. Thus, to understand why wider search angles yield faster extrusion in our simulations, we compute the success probability of making a step. Indeed, in our algorithm we impose that the LEF does not make a step if, in a given simulation time, there are no DNA beads that satisfy the search cri-

terion. This readily implies that narrower search angles yield lower success rates (Fig. 3d). The opposite trends of success rate (increasing with γ) and average step size (decreasing with γ) yield a trade-off (Fig. 3d) that naturally leads to an optimum in velocity around $\gamma \simeq 180^\circ$. However, we argue that condensin may employ a narrow angle to optimize the search process within a crowded DNA environment, within which the success probability would be generally larger.

Conclusions. – Motivated by AFM data, in this Letter we have provided experimental evidence that the structure of yeast condensin favours certain geometric conformations where the hinge is extended perpendicularly to the local direction of the heads-bound DNA segment. We have also quantified the width of the search angle, $\gamma = 60^\circ$ and computationally demonstrated that by imposing this geometric constraint, loop extrusion can be spontaneously rectified. Interestingly, we find that the narrower the search angle, the larger the typical the step size and the more unidirectional the extrusion, but also the more likely to fail to find a DNA segment to grab in a given time. This trade-off yields an optimum extrusion speed at a predicted angle of $\gamma = 180^\circ$.

We argue that the emergence of spontaneously rectified, unidirectional extrusion is due to a combination of

local deformations of the underlying DNA and the geometric constraint on the hinge-mediated 3D search. Our findings ought to be relevant to other SMC protein complexes, as long as their structure impose a geometric constraint on the conformational space of the DNA:protein complex. Additionally, they can reconcile a range of recent findings, e.g. bypassing of roadblocks, Z-loops, and also the pinching of a negatively supercoiled loop during the hinge-grabbing step [29], whilst also explaining the unidirectional extrusion. Our hypothesis could be tested by mutating the SMC coiled-coil arms to be more flexible or rigid, thereby directly increasing or reducing the search angle γ . Overall, we argue that our findings contribute to highlight a largely overlooked aspect of loop extrusion that ought to be relevant for the function of generic SMC complexes.

Acknowledgements. – DM acknowledges the Royal Society and the European Research Council (grant agreement No 947918, TAP) for funding. The authors also acknowledge the contribution of the COST Action Eutopia, CA17139. J.-K.R. acknowledges the Institute of Applied Physics of Seoul National University, Creative-Pioneering Researchers Program through Seoul National University (Project Number 3348-20230013), the Brain Korea 21 Four Project grant funded by the Korean Ministry of Education, Samsung Electronics Co., Ltd. (Project Number A0426-20220109), and the National Research Foundation of Korea (Project Number 0409-20230237, 0409-20230171, 0409-20230219).

* corresponding author, andrea.bonato@strath.ac.uk

† co-corresponding author, davide.michieletto@ed.ac.uk

‡ corresponding author, prof.love@snu.ac.kr

- [1] K. Nasmyth, *Nature Cell Biology* **13**, 1170 (2011).
- [2] E. Alipour and J. F. Marko, *Nucleic Acids Res.* **40**, 11202 (2012).
- [3] A. L. Sanborn, S. S. P. Rao, S.-C. Huang, N. C. Durand, M. H. Huntley, A. I. Jewett, I. D. Bochkov, D. Chinnappan, A. Cutkosky, J. Li, K. P. Geeting, A. Gnirke, A. Melnikov, D. McKenna, E. K. Stamenova, E. S. Lander, and E. L. Aiden, *Proc. Natl. Acad. Sci. USA* **112**, 201518552 (2015).
- [4] G. Fudenberg, M. Imakaev, C. Lu, A. Goloborodko, N. Abdennur, and L. A. Mirny, *Cell Reports* **15**, 2038 (2016).
- [5] T. Hirano, *Cell* **164**, 847 (2016).
- [6] I. F. Davidson and J. M. Peters, *Nature Reviews Molecular Cell Biology* **22**, 445 (2021).
- [7] S. Xiang and D. Koshland, *eLife* **10**, 1 (2021).
- [8] L. Vian, A. Pękowska, S. S. Rao, K. R. Kieffer-Kwon, S. Jung, L. Baranello, S. C. Huang, L. El Khattabi, M. Dose, N. Pruetz, A. L. Sanborn, A. Canela, Y. Maman, A. Oksanen, W. Resch, X. Li, B. Lee, A. L. Kovalchuk, Z. Tang, S. Nelson, M. Di Pierro, R. R. Cheng, I. Machol, B. G. St Hilaire, N. C. Durand, M. S. Shamim, E. K. Stamenova, J. N. Onuchic, Y. Ruan, A. Nussenzweig, D. Levens, E. L. Aiden, and R. Casellas, *Cell* **173**, 1165 (2018).
- [9] S. S. Rao, S.-C. Huang, B. G. S. Hilaire, J. M. Engreitz, E. M. Perez, K.-R. Kieffer-Kwon, A. L. Sanborn, S. E. Johnstone, G. D. Bascom, I. D. Bochkov, X. Huang, M. S. Shamim, J. Shin, D. Turner, Z. Ye, A. D. Omer, J. T. Robinson, T. Schlick, B. E. Bernstein, R. Casellas, E. S. Lander, and E. L. Aiden, *Cell* **171**, 305 (2017).
- [10] J. H. Gibcus, K. Samejima, A. Goloborodko, I. Samejima, N. Naumova, J. Nuebler, M. T. Kanemaki, L. Xie, J. R. Paulson, W. C. Earnshaw, L. A. Mirny, and J. Dekker, *Science* **359**, eaao6135 (2018).
- [11] I. A. Shaltiel, S. Datta, L. Lecomte, M. Hassler, M. Kschonsak, S. Bravo, C. Stober, J. Ormanns, S. Eustermann, and C. H. Haering, *Science* **376**, 1087 (2022).
- [12] T. L. Higashi, G. Pobegalov, M. Tang, M. I. Molodtsov, and F. Uhlmann, *eLife* **10**, 1 (2021).
- [13] S. K. Nomidis, E. Carlon, S. Gruber, and J. F. Marko, *Nucleic Acids Research* **50**, 4974 (2022).
- [14] R. Takaki, A. Dey, G. Shi, and D. Thirumalai, *Nature Communications* **12** (2021).
- [15] R. Barth, B. Pradhan, E. Kim, I. F. Davidson, J. van der Torre, J. M. Peters, and C. Dekker, *Scientific Reports* **13**, 1 (2023).
- [16] J. K. Ryu, A. J. Katan, E. O. van der Sluis, T. Wisse, R. de Groot, C. H. Haering, and C. Dekker, *Nature Structural and Molecular Biology* **27**, 1134 (2020).
- [17] B. W. Bauer, I. F. Davidson, D. Canena, G. Wutz, W. Tang, G. Litos, S. Horn, P. Hinterdorfer, and J. M. Peters, *Cell* **184**, 5448 (2021).
- [18] J. M. Eeftens, A. J. Katan, M. Kschonsak, M. Hassler, L. de Wilde, E. M. Dief, C. H. Haering, and C. Dekker, *Cell Reports* **14**, 1813 (2016).
- [19] A. Bonato and D. Michieletto, *Biophysical Journal* **120**, 5544 (2021).
- [20] E. Kim, J. Kerssemakers, I. A. Shaltiel, C. H. Haering, and C. Dekker, *Nature* **579**, 438 (2020).
- [21] H. B. Brandão, Z. Ren, X. Karaboja, L. A. Mirny, and X. Wang, *Nature Structural and Molecular Biology* **28**, 642 (2021).
- [22] H. B. Brandão, P. Paul, A. A. van den Berg, D. Z. Rudner, X. Wang, and L. A. Mirny, *Proceedings of the National Academy of Sciences of the United States of America* **116**, 20489 (2019).
- [23] B. Pradhan, R. Barth, E. Kim, I. F. Davidson, B. Bauer, T. van Laar, W. Yang, J. K. Ryu, J. van der Torre, J. M. Peters, and C. Dekker, *Cell Reports* **41**, 1 (2022).
- [24] M. Kschonsak, F. Merkel, S. Bisht, J. Metz, V. Rybin, M. Hassler, and C. H. Haering, *Cell* **171**, 588 (2017).
- [25] E. J. Banigan and L. A. Mirny, *Physical Review X* **9**, 031007 (2019).
- [26] E. Orlandini, D. Marenduzzo, and D. Michieletto, *Proceedings of the National Academy of Sciences* **116**, 8149 (2019).
- [27] J.-K. Ryu, S.-H. Rah, R. Janissen, J. W. J. Kerssemakers, A. Bonato, D. Michieletto, and C. Dekker, *Nucleic acids research* **50**, 820 (2022).
- [28] An alternative way to implement this constraints could be to impose a dihedral or angular potential between the DNA segments bound to heads and anchor. We expect to obtain similar results with this alternative implementation.
- [29] B. Martínez-García, S. Dyson, J. Segura, A. Ayats, E. E. Cutts, P. Gutierrez-Escribano, L. Aragón, and J. Roca, *The EMBO Journal* **42**, 1 (2023).